Journal of Southeast University (English Edition) Vol. 37, No. 4, pp. 356 - 364 Dec. 2021 ISSN 1003—7985

Calculation method for trajectory following control for autonomous vehicles

Wu Jianwei[1,2] Sun Beibei[1] Fu Qidi[1] Liu Yanhao[1]

([1]School of Mechanical Engineering, Southeast University, Nanjing 211189, China)

([2]School of Mechanical and Electrical Engineering, Guilin University of Electronic Technology, Guilin 541004, China)

Abstract: The current literature lacks uniform calculation methods for following trajectory control for autonomous vehicles, including the calculation of errors, determination of tracking points, and design of feedforward controllers. Hence, a complete calculation method is proposed to address this gap. First, a control equation in the form of an error is obtained according to the dynamic equation of the vehicle coordinate system and the trajectory following model. Secondly, the deviation of the vehicle state is obtained according to the current vehicle's state and the following control model. Finally, a linear quadratic regulator (LQR) controller with feedforward control is designed according to the characteristics of the dynamic equation. With the proposed LQR, the simulation of computational time, anti-interference, and reliability analysis of the trajectory following control is performed by programming using MATLAB. The simulation outcomes are then compared with the experimental results from the literature. The comparison indicates that the proposed complete calculation method is effective, reliable, and capable of achieving real-time and anti-interference following control performance. The simulation results with or without feedforward control show that the steady-state error is eliminated and that good control performance is obtained by introducing feedforward control.

Key words: trajectory following; autonomous vehicle; feedforward control; linear quadratic regulator (LQR)

DOI: 10.3969/j.issn.1003-7985.2021.04.003

With the development of advanced sensing and artificial intelligence techniques, autonomous vehicles are gaining increasing attention from the industry and academic communities and are regarded as the most promising industry for improving road safety in the future [1-3]. An autonomous vehicle is a highly integrated electromechanical coupling system comprising many vital technologies, such as car perception, image identification and processing, trajectory planning, trajectory following control, anti-lock brake, active suspension control technology, and automatic parking technologies. Trajectory following control, in particular, plays a vital role in the driving performances of autonomous vehicles. This technology is mainly aimed at tracking desired trajectories continuously and smoothly with the highest precision possible.

In the past decades, many studies have focused on trajectory following for autonomous vehicles. Specifically, these studies have mainly applied advanced control algorithms or proposed novel control algorithms so as to ensure driving safety and thereby achieve good control in situations in which vehicle models cannot be established accurately and uncertain external disturbances exist. At present, the control algorithms that are widely used in trajectory following control for autonomous vehicles include feedback linearization[4-5], sliding mode control[6-10], neural network control [11-13], and model predictive control [14-19].

Although a large number of studies in trajectory following for autonomous vehicles have been carried out, certain shortcomings remain. Most existing studies aimed to propose or use a new method from the control algorithm itself to show its outstanding performance by comparing it with other control methods. Only a few articles report calculation methods for trajectory following control that are detailed and complete, especially in terms of the calculation of errors, determination of tracking points, and design of feedforward controllers. For example, the work in Refs. [20-23] did not consider feedforward control in eliminating steady-state errors. Hence, the results are not useful in evaluating and fairly comparing the performance of control methods.

Accordingly, the current study presents a complete calculation method for trajectory following control for autonomous vehicles by calculating real-time tracking points on the basis of current vehicle states. The proposed method's implementation steps, in which computational equations are deduced by the dynamic equation of the global coordinate and control equation of trajectory following with an error form, are introduced systematically. A sample simulation of trajectory following control based on a linear

Received 2021-03-21, **Revised** 2021-06-23.

Biographies: Wu Jianwei (1989—), male, Ph. D. candidate; Sun Beibei (corresponding author), female, doctor, professor, bbSun@seu.edu.cn.

Foundation item: The National Key Research and Development Program of China (No. 2019YFB2006404), Guangxi Science and Technology Major Project (No. GUIKE AA18242036, No. GUIKE AA18242037).

Citation: Wu Jianwei, Sun Beibei, Fu Qidi, et al. Calculation method for trajectory following control for autonomous vehicles[J]. Journal of Southeast University (English Edition), 2021, 37(4): 356 - 364. DOI: 10.3969/j.issn.1003-7985.2021.04.003.

quadratic regulator (LQR) with a feedforward controller is performed by developing a program in MATLAB to facilitate the understanding of the calculation method. The implementation process and simulation results are described accordingly. Computational cost and reliability analyses are also performed.

1 Vehicle Dynamical Modeling for Trajectory Following Control

The vehicle handling dynamics model using three degrees of freedom (DOF) essentially describes trajectory following control. To facilitate the description of the calculation method for trajectory following control, this work makes the following main assumptions: 1) The differences in the tire cornering properties between the left and right wheels due to load variation are ignored, and the tire model is approximated as linear; 2) The vehicle only executes front-wheel steering; 3) Longitudinal velocity is a constant value. The vehicle dynamical model is shown in Fig. 1, where *OXYZ* represents the global coordinate system and *Cxyz* represents the vehicle coordinate system whose origin is the vehicle centroid and the *x*-axis is the driving direction.

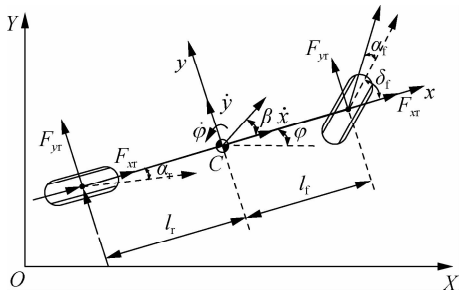

Fig. 1 Vehicle dynamical model

1.1 Dynamical equation under the vehicle coordinate system

In the maneuvering dynamical model, the external force transmitted by the tire to the vehicle primarily depends on the speed variable rather than on the absolute position coordinates and heading angle of the vehicle. Therefore, the dynamical equation is established using the coordinate system *Cxyz* fixed on the vehicle. According to the assumption that the longitudinal velocity is constant, the dynamical equation can be obtained as [8, 16]

$$\begin{bmatrix} \dot{y} \\ \ddot{y} \\ \dot{\varphi} \\ \ddot{\varphi} \end{bmatrix} = \begin{bmatrix} 0 & 1 & 0 & 0 \\ 0 & -\dfrac{2C_{\alpha f}+2C_{\alpha r}}{mV_x} & 0 & \dfrac{-2l_f C_{\alpha f}+2l_r C_{\alpha r}}{mV_x}-V_x \\ 0 & 0 & 0 & 1 \\ 0 & -\dfrac{2l_f C_{\alpha f}-2l_r C_{\alpha r}}{I_z V_x} & 0 & -\dfrac{2l_f^2 C_{\alpha f}+2l_r^2 C_{\alpha r}}{I_z V_x} \end{bmatrix} \cdot \begin{bmatrix} y \\ \dot{y} \\ \varphi \\ \dot{\varphi} \end{bmatrix} + \begin{bmatrix} 0 \\ \dfrac{2C_{\alpha f}}{m} \\ 0 \\ \dfrac{2l_f C_{\alpha f}}{I_z} \end{bmatrix} \delta_f \tag{1}$$

where y is the lateral displacement; $\dot{y}$ is the lateral velocity; φ is the yaw angle; $\dot{\varphi}$ is the yaw rate; m is the total vehicle mass; I_z represents the vehicle inertia around the axis C_z; V_x is the longitudinal velocity; δ_f is the front steering angle; l_f and l_r denote the distances between the front and rear wheel axles with C, respectively; and $C_{\alpha f}$ and $C_{\alpha r}$ represent the front and rear cornering stiffness, respectively.

1.2 Dynamical equation under the global coordinate system

When performing trajectory following control in an actual road, an autonomous vehicle needs to accurately measure and estimate the current vehicle states, such as the yaw rate, longitudinal velocity, and lateral velocity, by utilizing a GPS/INS navigation system [21]. Similarly, an autonomous vehicle needs to obtain these states by using the dynamical equation on the global coordinate system when performing simulation control for trajectory following. An increasing number of studies have adopted the multibody dynamical model on the basis of dynamic software, such as ADAMS, SIMPACK, and CarSim, to compute vehicle states accurately.

As the current work mainly focuses on the calculation method for trajectory following, a 3-DOF dynamical model is employed for computing vehicle states. According to the momentum and moment of momentum theorem under the assumption of constant longitudinal velocity, the dynamical equation on the global coordinate system can be obtained as

$$m\ddot{X} = -2F_{yf}\sin(\varphi) - 2F_{yr}\sin(\varphi) \tag{2}$$

$$m\ddot{Y} = 2F_{yf}\cos(\varphi) + 2F_{yr}\cos(\varphi) \tag{3}$$

$$I_z\ddot{\varphi} = 2(aF_{yf} - bF_{yr}) \tag{4}$$

where X and Y represent the vehicle's center-of-mass coordinate with respect to *OXYZ*; φ represents the attitude of *oxyz* with respect to *OXYZ* (i.e., yaw angle of the vehicle); and F_{yf} and F_{yr} denote the y-axis component of the front and rear lateral tire forces with respect to *oxyz*, respectively.

The transformation relationship between *oxyz* and *OXYZ* is given by

$$\begin{bmatrix} \dot{x} \\ \dot{y} \end{bmatrix} = \begin{bmatrix} \cos(\varphi) & \sin(\varphi) \\ -\sin(\varphi) & \cos(\varphi) \end{bmatrix} \begin{bmatrix} \dot{X} \\ \dot{Y} \end{bmatrix} \tag{5}$$

F_{yf} and F_{yr} are respectively calculated by the tire side-slip

characteristics as

$$F_{yf} = C_{\alpha f}\left(\delta_f - \frac{\dot{y} + l_f\dot{\varphi}}{V_x}\right) \tag{6}$$

$$F_{yr} = C_{\alpha r}\left(-\frac{\dot{y} - l_r\dot{\varphi}}{V_x}\right) \tag{7}$$

The dynamical equations under the global coordinate system can be obtained by substituting Eqs. (5) to (7) into Eqs. (2) to (4).

1.3 Control equation with error form

The vehicle trajectory following model is shown in Fig. 2, where C_d is the desired position and C is the real position of the vehicle's center of mass. In Fig. 2, point C_d is on the desired trajectory, and vector CC_d and the tangent of C_d are perpendicular. The desired coordinate system $C_d x_d y_d z_d$ can be defined as follows: the tangent of C_d is the x-axis, and vector $C_d C$ is the y-axis. In Fig. 2, φ_{des} and $\dot{\varphi}_{des}$ respectively represent the desired yaw angle and yaw rate of the vehicle; V_{xdes} represents the desired longitudinal velocity; and V_x, $\dot{y}$, $\ddot{y}$, φ, $\dot{\varphi}$, and $\ddot{\varphi}$ respectively denote the actual longitudinal velocity, lateral velocity, lateral acceleration, yaw angle, yaw rate, and angular acceleration of the vehicle. The magnitudes of V_{xdes} and V_x are equal, but their directions are different.

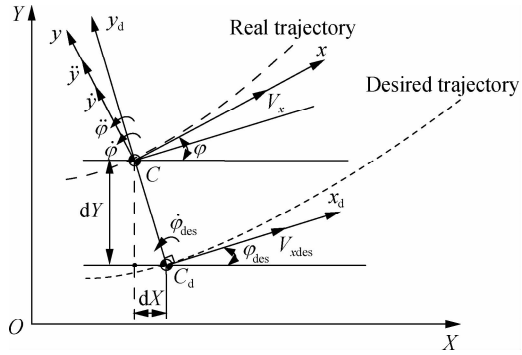

Fig. 2 Trajectory following model

Transforming the states into the same coordinate system is necessary to obtain the errors between actual states and desired states. After performing the projection operation of the states into the desired coordinate system, the error between the actual and desired lateral accelerations can be expressed as

$$\dot{e}_y = (\ddot{y} + \dot{\varphi}V_x)\cos(\varphi - \varphi_{des}) - \dot{\varphi}\dot{y}\sin(\varphi - \varphi_{des}) - \dot{\varphi}_{des}V_{xdes} \tag{8}$$

The error between the actual lateral and the desired lateral velocities is given by

$$\dot{e}_y = \dot{y}\cos(\varphi - \varphi_{des}) + V_x\sin(\varphi - \varphi_{des}) \tag{9}$$

As the value of $\varphi - \varphi_{des}$ is extremely small, $\dot{y}$ is far less than V_x, and the magnitudes of V_x and V_{des} are equal. Therefore, Eqs. (8) and (9) can be simplified as

$$\dot{e}_y = \ddot{y} + V_x(\dot{\varphi} - \dot{\varphi}_{des}) \tag{10}$$

$$\dot{e}_y = \dot{y} + V_x(\varphi - \varphi_{des}) \tag{11}$$

The error between the actual and desired yaw angles is defined as

$$e_\varphi = \varphi - \varphi_{des} \tag{12}$$

The error between the actual yaw rate and the desired yaw rate is given as

$$\dot{e}_\varphi = \dot{\varphi} - \dot{\varphi}_{des} \tag{13}$$

By substituting Eqs. (10) to (13) into Eq. (1), the dynamical equation with the error form can be obtained as

$$\dot{\boldsymbol{e}} = \boldsymbol{A}\boldsymbol{e} + \boldsymbol{B}\delta_f + \boldsymbol{C}\dot{\varphi}_{des} \tag{14}$$

where

$$\boldsymbol{e} = \begin{bmatrix} e_y \\ \dot{e}_y \\ e_\varphi \\ \dot{e}_\varphi \end{bmatrix},\quad \boldsymbol{B} = \begin{bmatrix} 0 \\ \dfrac{2C_{\alpha f}}{m} \\ 0 \\ \dfrac{2l_fC_{\alpha f}}{I_z} \end{bmatrix},\quad \boldsymbol{C} = \begin{bmatrix} 0 \\ \dfrac{-2l_fC_{\alpha f} + 2l_rC_{\alpha r}}{mV_x} - V_x \\ 0 \\ -\dfrac{2l_f^2C_{\alpha f} + 2l_r^2C_{\alpha r}}{I_zV_x} \end{bmatrix}$$

$$\boldsymbol{A} = \begin{bmatrix} 0 & 1 & 0 & 0 \\ 0 & -\dfrac{2C_{\alpha f} + 2C_{\alpha r}}{mV_x} & \dfrac{2C_{\alpha f} + 2C_{\alpha r}}{m} & \dfrac{-2l_fC_{\alpha f} + 2l_rC_{\alpha r}}{mV_x} \\ 0 & 0 & 0 & 1 \\ 0 & -\dfrac{2l_fC_{\alpha f} - 2l_rC_{\alpha r}}{I_zV_x} & \dfrac{2l_fC_{\alpha f} - 2l_rC_{\alpha r}}{I_z} & -\dfrac{2l_f^2C_{\alpha f} + 2l_r^2C_{\alpha r}}{I_zV_x} \end{bmatrix}$$

2 Calculation Method for Trajectory Following Control

With a plan for the desired trajectory in place, trajectory following control is aimed toward driving the vehicle along such trajectory as closely as possible. Control algorithms include PID control, LQR control, sliding mode control, and fuzzy neural network control. In the current work, the LQR method, which is one of the most representative control methods, is adopted to facilitate the understanding of the calculation method for trajectory following control.

To realize trajectory following control, this study proposes the following six steps:

Step 1 Plan the desired trajectory according to the driving purpose.

Step 2 Obtain the current vehicle states, such as actual position, longitudinal velocity, lateral velocity, yaw angle, and yaw rate, on the basis of the vehicle dynamical model or vehicle perception equipment.

Step 3 Determine the desired point states and their deviations between the actual point and the tracking point according to the current vehicle states and the desired traj-

ectory.

Step 4 Calculate the control input on the basis of the control equation with the error form, feedforward control, and LQR control method.

Step 5 Obtain the actual vehicle position, longitudinal velocity, lateral velocity, yaw angle, and yaw rate at the next moment by using the vehicle simulation model after inputting the control quantity obtained from step 4.

Step 6 Repeat steps 2 to 5 until the end.

2.1 Planning the desired trajectory

Several geometric forms can be used to plan the following trajectory. In particular, polynomial trajectories are the most common form used in automated driving [24-26]. In this work, the following cubic polynomial is adopted to express the desired trajectory:

$$Y = f(X) = a_3X^3 + a_2X^2 + a_1X^1 + a_0 \tag{15}$$

where a_0 to a_3 are the fit coefficients of the cubic polynomial.

2.2 Calculating errors between desired and actual states

The assumption is that vehicle states $(X(t), Y(t), \varphi(t), \dot{X}(t), \dot{Y}(t), \dot{\varphi}(t))$ at moment t have been obtained on the basis of the vehicle dynamical model. The following five calculation steps are given for calculating the desired states and actual errors at moment t:

1) Calculate $X_{\mathrm{des}}(t)$ and $Y_{\mathrm{des}}(t)$. According to the actual point $C[X(t), Y(t)]$ from the vehicle's center of mass, calculate tracking point C_{d} with trajectory function $y = f(x)$. The straight line CC_{d} and tangent of C_{d} satisfy

$$(Y(t) - f(X_{\mathrm{des}}(t)))f'(X_{\mathrm{des}}(t)) + X(t) - X_{\mathrm{des}}(t) = 0 \tag{16}$$

$X_{\mathrm{des}}(t)$ can be easily obtained by solving the algebraic Eq. (16) while considering $X(t)$ as the initial point. Then, $Y_{\mathrm{des}}(t)$ can be acquired by trajectory function $y = f(x)$.

2) Calculate $\varphi_{\mathrm{des}}(t)$. In accordance with $X_{\mathrm{des}}(t)$ and trajectory function $y = f(x)$, $\varphi_{\mathrm{des}}(t)$ is given as

$$\varphi_{\mathrm{des}}(t) = \arctan f(X_{\mathrm{des}}(t)) \tag{17}$$

3) Determine $\dot{\varphi}_{\mathrm{des}}(t)$. With the curvature radius formula, the curvature of point C_{d} is given as

$$\kappa(t) = \frac{f'(X_{\mathrm{des}}(t))}{(1 + (f'(X_{\mathrm{des}}(t)))^2)^{3/2}} \tag{18}$$

Then, the desired yaw rate at moment t is calculated as

$$\dot{\varphi}_{\mathrm{des}}(t) = V_x\kappa(t) \tag{19}$$

4) Calculate $e_y(t)$ and $\dot{e}_y(t)$. By transforming the actual and desired points into the desired coordinate system $C_{\mathrm{d}}x_{\mathrm{d}}y_{\mathrm{d}}z_{\mathrm{d}}$, $e_y(t)$ and $\dot{e}_y(t)$ can be respectively calculated as

$$e_y(t) = -(X(t) - X_{\mathrm{des}}(t))\sin(\varphi_{\mathrm{des}}(t)) + (Y(t) - Y_{\mathrm{des}}(t))\cos(\varphi_{\mathrm{des}}(t)) \tag{20}$$

$$\dot{e}_y(t) = -\dot{X}(t)\sin(\varphi_{\mathrm{des}}(t)) + \dot{Y}(t)\cos(\varphi_{\mathrm{des}}(t)) \tag{21}$$

5) Obtain $e_\varphi(t)$ and $\dot{e}_\varphi(t)$, according to Eqs. (12) and (13).

2.3 Determining the control input

According to Eq. (14) and the LQR method, the control input $\delta_{\mathrm{f}_1}(t)$ is obtained as

$$\delta_{\mathrm{f1}}(t) = -\boldsymbol{K}\left[\, e_y(t) \quad \dot{e}_y(t) \quad e_\varphi(t) \quad \dot{e}_\varphi(t) \,\right]^{\mathrm{T}} \tag{22}$$

where $\boldsymbol{K}$ is the feedback gain matrix of the optimal control and can be expressed as

$$\boldsymbol{K} = \boldsymbol{R}^{-1}\boldsymbol{B}^{\mathrm{T}}\boldsymbol{P} \tag{23}$$

where $\boldsymbol{P}$ can be obtained by the Riccati equation, which has the following form:

$$\boldsymbol{P}\boldsymbol{A} + \boldsymbol{A}^{\mathrm{T}}\boldsymbol{P} - \boldsymbol{P}\boldsymbol{B}\,\boldsymbol{R}^{-1}\boldsymbol{B}^{\mathrm{T}}\boldsymbol{P} + \boldsymbol{Q} = \boldsymbol{0} \tag{24}$$

where $\boldsymbol{R}$ is the weight matrix on the control input and $\boldsymbol{Q}$ is the weight matrix on the error.

As the variation of the desired angular velocity results from the different curvatures of the desired trajectory at different times, a feedforward controller is adopted to minimize tracking errors and ensure zero steady-state errors. The autonomous vehicle with only front wheel steering belongs to the under-actuated control system, which cannot completely eliminate the steady-state errors from the two states. Nevertheless, we can ensure zero lateral steady-state error, which is more important than angular steady-state error.

Therefore, the feedforward controller—used for completely eliminating the lateral steady-state error—is introduced in detail. However, an angular steady-state error still exists in the under-actuated control system. According to feedback gain matrix $\boldsymbol{K}$, the closed-loop matrix $\boldsymbol{A}_{\mathrm{b}}$ can be expressed as

$$\boldsymbol{A}_{\mathrm{b}} = \boldsymbol{A} - \boldsymbol{B}\boldsymbol{K} \tag{25}$$

As the first and third rows of $\boldsymbol{B}$ are zero, $\boldsymbol{A}_{\mathrm{b}}$ is always satisfied as follows, regardless of the value of $\boldsymbol{K}$:

$$\boldsymbol{A}_{\mathrm{b}}(1,1) = \boldsymbol{A}_{\mathrm{b}}(1,3) = \boldsymbol{A}_{\mathrm{b}}(1,4) = 0, \quad \boldsymbol{A}_{\mathrm{b}}(1,2) = 1 \tag{26}$$

$$\boldsymbol{A}_{\mathrm{b}}(3,1) = \boldsymbol{A}_{\mathrm{b}}(3,2) = \boldsymbol{A}_{\mathrm{b}}(3,3) = 0, \quad \boldsymbol{A}_{\mathrm{b}}(3,4) = 1 \tag{27}$$

Hence, on the basis of Eq. (14) and $\dot{e}_{ys}(t) = \dot{e}_{\varphi s}(t) = 0$, the relationship between the steady-state error and the feedforward control can be written as the following matrix equation:

$$\begin{bmatrix} \boldsymbol{A}_b(2,1) & \boldsymbol{A}_b(2,3) \\ \boldsymbol{A}_b(4,1) & \boldsymbol{A}_b(4,3) \end{bmatrix} \begin{bmatrix} e_{ys}(t) \\ e_{\varphi s}(t) \end{bmatrix} + \begin{bmatrix} \boldsymbol{B}(2)\delta_{f2}(t) + \boldsymbol{C}(2)\dot{\varphi}_{des}(t) \\ \boldsymbol{B}(4)\delta_{f2}(t) + \boldsymbol{C}(4)\dot{\varphi}_{des}(t) \end{bmatrix} = \begin{bmatrix} 0 \\ 0 \end{bmatrix} \tag{28}$$

where $e_{ys}(t)$ and $e_{\varphi s}(t)$ respectively denote the lateral and angular steady-state errors at moment t.

After ensuring $e_{ys}(t) = 0$, the steady-state angular error and feedforward control quantity at moment t can be expressed as the following matrix equation:

$$\begin{bmatrix} e_{\varphi s}(t) \\ \delta_{f2}(t) \end{bmatrix} = -\begin{bmatrix} \boldsymbol{A}_b(2,3) & \boldsymbol{B}(2) \\ \boldsymbol{A}_b(4,3) & \boldsymbol{B}(4) \end{bmatrix}^{-1} \begin{bmatrix} \boldsymbol{C}(2) \\ \boldsymbol{C}(4) \end{bmatrix} \dot{\varphi}_{des}(t) \tag{29}$$

By combining the LQR with the feedforward control, the total control input can be calculated as

$$\delta_f(t) = \delta_{f1}(t) + \delta_{f2}(t) \tag{30}$$

As a result of the demand for vehicle safety and physical implementation, the control input is not completely determined by Eq. (30), and the value range needs to be considered. Herein, the ranges of the front steering angle and front steering angle velocity are respectively given by

$$\delta_{min} \leqslant \delta_f(t) \leqslant \delta_{max} \tag{31}$$

$$\dot{\delta}_{min} \leqslant \frac{\delta_f(t) - \delta_f(t - \Delta t)}{\Delta t} \leqslant \dot{\delta}_{max} \tag{32}$$

where δ_{min} and δ_{max} represent the maximum and minimum values of the front steering angle, respectively; and $\dot{\delta}_{min}$ and $\dot{\delta}_{max}$ represent the maximum and minimum values of the front steering angle velocity, respectively.

2.4 Vehicle dynamics simulation under control input

The next moment vehicle states—$X(t+\Delta t)$, $Y(t+\Delta t)$, $\varphi(t+\Delta t)$, $\dot{X}(t+\Delta t)$, $\dot{Y}(t+\Delta t)$, and $\dot{\varphi}(t+\Delta t)$—can be calculated according to the vehicle dynamical model in Section 1.2 and the control input obtained by Section 2.3. By repeating the steps detailed in Sections 2.2, 2.3, and 2.4 until the end, the simulation results for trajectory following control can be obtained.

3 Simulation and Analysis

A program is independently developed in MATLAB to evaluate the feasibility and effectiveness of the proposed calculation method in Section 2. The developed program is used to implement the trajectory following control simulation.

3.1 Desired trajectory

The desired trajectory adopts the polynomial expression where $a_0 = 0$, $a_1 = 0.999\ 886\ 710\ 218\ 506$, $a_2 = -0.004\ 998\ 300\ 653\ 278$, and $a_3 = -0.566\ 448\ 9 \times 10^{-8}$, as shown in Fig. 3. The desired trajectory has a minimum curvature radius of 100 mm. The control effect of trajectory following is known to depend largely on the curvature radius of the desired trajectory. In other words, the smaller the curvature radius is, the harder the control becomes. Following this trajectory under the longitudinal velocity of 10 m/s is relatively difficult, but this trajectory has certain representativeness.

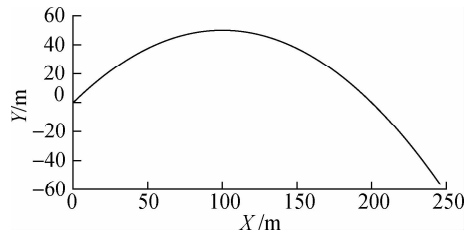

Fig. 3 Desired trajectory curve

3.2 Vehicle simulation parameters

The simulation parameters are shown in Tab. 1.

Tab. 1 Simulation parameters of the vehicle model

Parameter	Value
Vehicle mass m/kg	1 575
Vehicle yaw moment I_z/(kg · m^2)	2 875
Front-CG distance l_f/m	1.2
Rear-CG distance l_r/m	1.6
Cornering stiffness of front tires C_f/(kN · rad^{-1})	19
Cornering stiffness of rear tires C_r/(kN · rad^{-1})	33
Maximum steering angle δ_{max}/rad	0.523 6
Minimum steering angle δ_{min}/rad	−0.523 6
Maximum steering angle velocity $\dot{\delta}_{max}$/(rad · s^{-1})	0.261 8
Minimum steering angle velocity $\dot{\delta}_{min}$/(rad · s^{-1})	−0.261 8
Longitudinal velocity V_x/(m · s^{-1})	10

3.3 Simulation results and analysis

The initial states are defined as follows: The yaw angle of the vehicle relative to the global coordinate system is 0.785 3 rad, the yaw rate is 0 rad/s, the longitudinal velocity is 10 m/s, and the lateral velocity is 0 m/s. The global coordinate of the vehicle's center of mass is (0, 1) m. In the initial states, the simulation time is set to 30 s, and the simulation results of the trajectory following control are shown in Figs. 4 to 6.

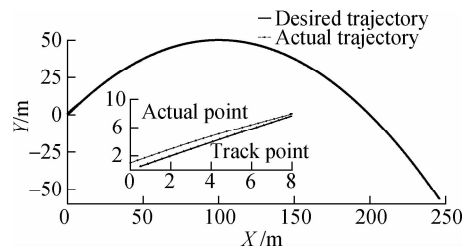

Fig. 4 Contrast between desired and actual trajectories

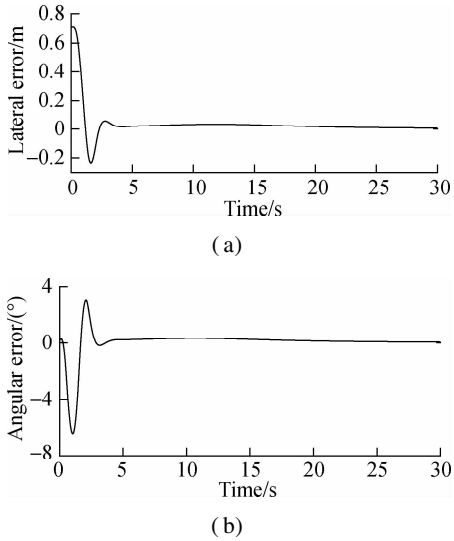

Fig. 5 Response of error. (a) Lateral error; (b) Angular error

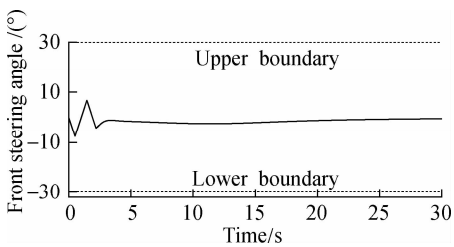

Fig. 6 Response of front steering angle

Fig. 4 shows the tracking process from the actual vehicle position to the desired trajectory position. The simulation presents a good trajectory following effect, and the actual vehicle position fluctuates around the desired trajectory at a small-scale level. The standard deviation between the actual trajectory and the desired trajectory is calculated as 0.11 m.

Fig. 5 presents the error responses. The lateral and angular errors gradually decrease by controlling the front steering angle, which achieves the desired control effect. Furthermore, the steady-state errors gradually tend to approach zero because of the introduction of feedforward control. As illustrated in Fig. 5 (a), the lateral steady-state error can be completely eliminated, although the trajectory curvature is not zero. The simulation results also reveal that when the vehicle passes through the position with a relatively large curvature, the tracking effect deteriorates to a certain extent despite the introduction of feedforward control.

Fig. 6 shows the response of the front steering angle provided by the LQR controller with feedforward control. The front steering angle is limited to the given range, which meets the requirements of the vehicle's physical realizability. In addition, the front steering angle is much smaller than the given boundary value, and the variation range of the angle is small. These features can strongly guarantee vehicle safety.

For the purpose of illustrating the strong anti-interference ability of the proposed method that calculates trace points in real-time on the basis of current vehicle states, an accidental interference in 7.5 s is assumed to cause large deviations (0.5 m, 0.5 m, 0.1 rad) between the actual vehicle position and the calculated position. Figs. 7 and 8 show the responses of the error and front steering angle. After being greatly disturbed in 7.5 s, the system automatically adjusts the trace point to eliminate the deviation according to the current actual states so that the vehicle drives along the desired trajectory and achieves a good control effect.

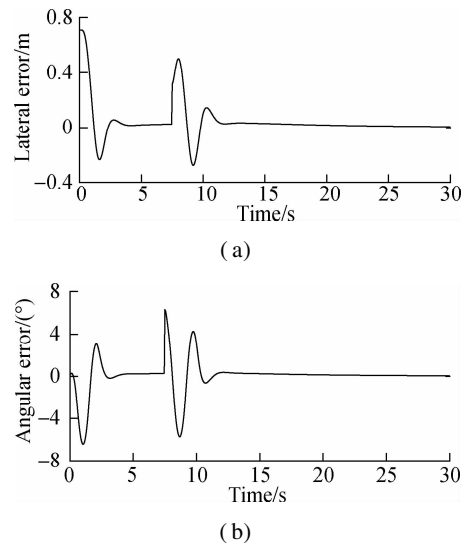

Fig. 7 Response of error with accidental interference. (a) Lateral error; (b) Angular error

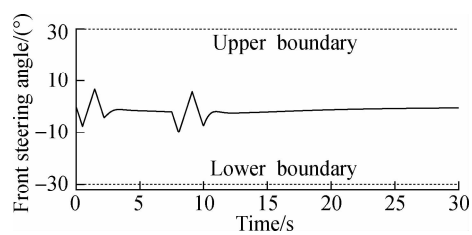

Fig. 8 Response of front steering angle with accidental interference

3.4 Computational cost

Computational cost is a crucial factor that determines whether the proposed algorithm can be used in practice. Hence, it requires evaluation. The computer configurations for the simulation are as follows: Windows 10 64-bit operating system, AMD Ryzen 7 CPU, 16 GB RAM with 3 200 MHz, and MATLAB version R2018a.

Under this computing environment, the computation time can be obtained by using a timer. When the simulation time is set to 30 s, the computation time is 0.56 s, which is the average time for 20 repetitions. Furthermore, the timer indicates that the computational cost

mainly depends on "fsolve" [i. e., the solution of algebraic Eq. (16)]. Nevertheless, the computation time is so small that the real-time performance is generally easy to satisfy under the computing environment. The algorithm can be further optimized in the future, particularly in terms of the calculation of the tracking point.

4 Reliability Analysis and Discussion by Experimental Comparison

The simulation results based on the proposed calculation method and the experimental results from Ref. [21] are compared under the same vehicle parameters and tracking trajectory to further analyze the reliability of the simulation results. The tracking trajectory is defined as trajectory 1. The simulation parameters of the experimental vehicle are not given in the literature, but after a careful search [12], the vehicle parameters are established. Meanwhile, Gaussian noise considering sensor accuracy is added to the vehicle state in the simulation to effectively reflect the actual states of the vehicle. The coordinate axis and its range are unified to ensure a good comparison with the results from the literature (see Figs. 9 to 12).

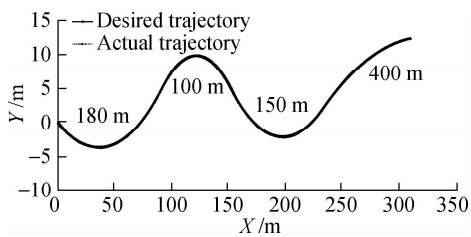

(a)

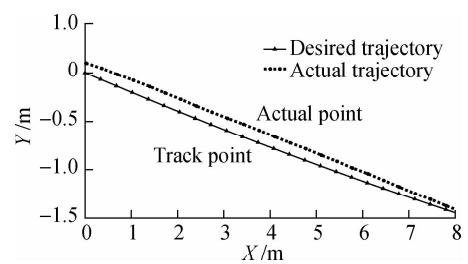

(b)

Fig. 9 Desired trajectory and actual trajectory based on trajectory 1. (a) Global view at 0 to 320 m; (b) Partial enlarged view at 0 to 8 m

For clarity, an enlarged view at 0-8 m is shown in Fig. 9 (b). Fig. 9 shows that good tracking performance is achieved.

Feedforward control is not considered in eliminating the steady-state error in this study. The dotted curves in Figs. 10 to 12 show the counterparts without the feedforward controller (i. e., no δ_{f2}). Relative to this literature, the simulation results without the feedforward controller (see Figs. 10 to 12) are consistent with the experimental results. The simulation results of yaw rate and front steering angle, in particular, are nearly identical to the experimental results. Hence, the simulation results are reliable, and the proposed calculation method is feasible.

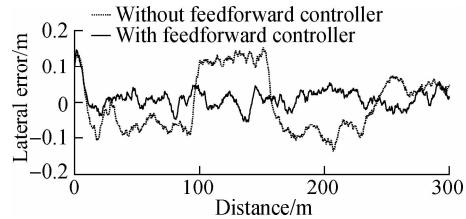

(a)

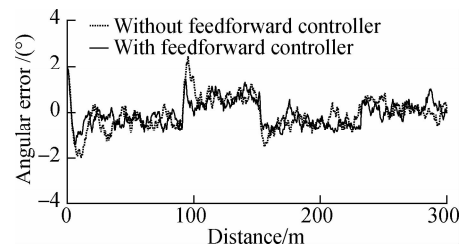

(b)

Fig. 10 Response of error based on trajectory 1. (a) Lateral error; (b) Angular error

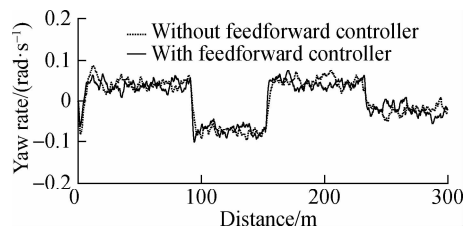

Fig. 11 Response of yaw rate based on trajectory 1

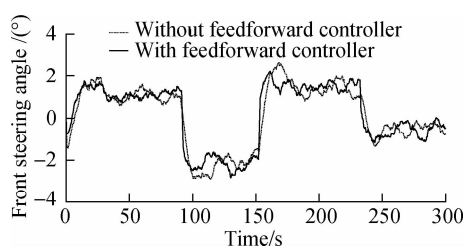

Fig. 12 Response of front steering angle based on trajectory 1

According to the complete calculation method proposed in this work, the feedforward controller should also be considered to obtain good control performance. The solid curves in Figs. 10 to 12 show the simulation results with the feedforward controller. The lateral steady-state error can be adjusted to zero while the changes in the angular error, yaw rate, and front steering angle are not apparent. After careful observation (see Figs. 10 to 12), the angular error, yaw rate, and front wheel angle are slightly smaller than their counterparts in the case without the feedforward controller. Hence, a good control effect is achieved with the complete calculation method for trajectory following control despite the control method being traditional.

5 Conclusions

1) A complete calculation method is proposed for the trajectory following control of autonomous vehicles. The implementation steps are also systematically introduced. The feedforward controller with LQR is designed for completely eliminating lateral steady-state errors according to the characteristics of the dynamical equation.

2) A program is independently developed in MATLAB, and a sample simulation is performed. The simulation results show that the control strategies based on the proposed calculation method achieve strong tracking and anti-interference performance.

3) The simulation results are determined to be reliable, and the proposed calculation method is deemed feasible by comparing the experimental results from the literature. In addition, good control performance is achieved with the proposed complete calculation method for trajectory following control, particularly through the introduction of the feedforward controller.

References

[1] Luo Y G, Xiang Y, Cao K, et al. A dynamic automated lane change maneuver based on vehicle-to-vehicle communication[J]. *Transportation Research Part C: Emerging Technologies*, 2016, **62**: 87 - 102. DOI: 10.1016/j.trc.2015.11.011.

[2] Li X H, Sun Z P, Cao D P, et al. Development of a new integrated local trajectory planning and tracking control framework for autonomous ground vehicles[J]. *Mechanical Systems and Signal Processing*, 2017, **87**: 118 - 137. DOI: 10.1016/j.ymssp.2015.10.021.

[3] Amer N H, Zamzuri H, Hudha K, et al. Modelling and control strategies in path tracking control for autonomous ground vehicles: A review of state of the art and challenges[J]. *Journal of Intelligent & Robotic Systems*, 2017, **86**(2): 225 - 254. DOI: 10.1007/s10846-016-0442-0.

[4] Javid S, Eghtesad M, Khayatian A, et al. Experimental study of dynamic based feedback linearization for trajectory tracking of a four-wheel autonomous ground vehicle [J]. *Autonomous Robots*, 2005, **19**(1): 27 - 40. DOI: 10.1007/s10514-005-0604-6.

[5] Dekker L G, Marshall J A, Larsson J. Experiments in feedback linearized iterative learning-based path following for center-articulated industrial vehicles[J]. *Journal of Field Robotics*, 2019, **36**(5): 955 - 972. DOI: 10.1002/rob.21864.

[6] Taghia J, Wang X, Lam S, et al. A sliding mode controller with a nonlinear disturbance observer for a farm vehicle operating in the presence of wheel slip[J]. *Autonomous Robots*, 2017, **41**(1): 71 - 88. DOI: 10.1007/s10514-015-9530-4.

[7] Hu C, Wang R R, Yan F J. Integral sliding mode-based composite nonlinear feedback control for path following of four-wheel independently actuated autonomous vehicles [J]. *IEEE Transactions on Transportation Electrification*, 2016, **2**(2): 221 - 230. DOI: 10.1109/TTE.2016.2537046.

[8] Xu L H, Wang Y Z, Sun H B, et al. Integrated longitudinal and lateral control for kuafu-Ⅱ autonomous vehicle [J]. *IEEE Transactions on Intelligent Transportation Systems*, 2016, **17**(7): 2032 - 2041. DOI: 10.1109/TITS.2015.2498170.

[9] Kayacan E, Kayacan E, Ramon H, et al. Towards agrobots: Trajectory control of an autonomous tractor using type-2 fuzzy logic controllers[J]. *IEEE/ASME Transactions on Mechatronics*, 2015, **20**(1): 287 - 298. DOI: 10.1109/TMECH.2013.2291874.

[10] Chebly A, Talj R, Charara A. Coupled longitudinal/lateral controllers for autonomous vehicles navigation, with experimental validation[J]. *Control Engineering Practice*, 2019, **88**: 79 - 96. DOI: 10.1016/j.conengprac.2019.05.001.

[11] Han G N, Fu W P, Wang W, et al. The lateral tracking control for the intelligent vehicle based on adaptive PID neural network[J]. *Sensors (Basel, Switzerland)*, 2017, **17**(6): E1244. DOI: 10.3390/s17061244.

[12] Guo J H, Luo Y G, Li K Q. Adaptive coordinated collision avoidance control of autonomous ground vehicles[J]. *Proceedings of the Institution of Mechanical Engineers, Part Ⅰ: Journal of Systems and Control Engineering*, 2018, **232**(9): 1120 - 1133. DOI: 10.1177/0959651818774991.

[13] Chen Y M, Lu C, Chu W B. A cooperative driving strategy based on velocity prediction for connected vehicles with robust path-following control[J]. *IEEE Internet of Things Journal*, 2020, **7**(5): 3822 - 3832. DOI: 10.1109/JIOT.2020.2969209.

[14] Luan Z K, Zhang J N, Zhao W Z, et al. Trajectory tracking control of autonomous vehicle with random network delay[J]. *IEEE Transactions on Vehicular Technology*, 2020, **69**(8): 8140 - 8150. DOI: 10.1109/TVT.2020.2995408.

[15] Yin G D, Li J H, Jin X J, et al. Integration of motion planning and model-predictive-control-based control system for autonomous electric vehicles[J]. *Transport*, 2015, **30**(3): 353 - 360. DOI: 10.3846/16484142.2015.1089322.

[16] Yakub F, Mori Y. Comparative study of autonomous path-following vehicle control via model predictive control and linear quadratic control[J]. *Proceedings of the Institution of Mechanical Engineers, Part D: Journal of Automobile Engineering*, 2015, **229**(12): 1695 - 1714. DOI: 10.1177/0954407014566031.

[17] Kayacan E, Ramon H, Saeys W. Robust trajectory tracking error model-based predictive control for unmanned ground vehicles[J]. *IEEE/ASME Transactions on Mechatronics*, 2016, **21**(2): 806 - 814. DOI: 10.1109/TMECH.2015.2492984.

[18] Ji J, Khajepour A, Melek W W, et al. Path planning and tracking for vehicle collision avoidance based on model predictive control with multiconstraints[J]. *IEEE Transactions on Vehicular Technology*, 2017, **66**(2): 952 - 964. DOI: 10.1109/TVT.2016.2555853.

[19] Hu J J, Xiong S S, Zha J L, et al. Lane detection and trajectory tracking control of autonomous vehicle based on model predictive control[J]. *International Journal of Au-*

tomotive Technology, 2020, **21**(2): 285 - 295. DOI: 10.1007/s12239-020-0027-6.

[20] Yao T. A model predictive controller with longitudinal speed compensation for autonomous vehicle path tracking [J]. *Applied Sciences*, 2019, **9**(22): 4739. DOI: 10.3390/app9224739.

[21] Guo J H, Luo Y G, Li K Q. An adaptive hierarchical trajectory following control approach of autonomous four-wheel independent drive electric vehicles[J]. *IEEE Transactions on Intelligent Transportation Systems*, 2018, **19**(8): 2482 - 2492. DOI: 10.1109/TITS.2017.2749416.

[22] Guo J H, Li K Q, Luo Y G. Coordinated control of autonomous four wheel drive electric vehicles for platooning and trajectory tracking using a hierarchical architecture [J]. *Journal of Dynamic Systems, Measurement, and Control*, 2015, **137**(10): 101001. DOI: 10.1115/1.4030720.

[23] Sun C Y, Zhang X, Xi L H, et al. Design of a path-tracking steering controller for autonomous vehicles[J]. *Energies*, 2018, **11**(6): 1451. DOI: 10.3390/en11061451.

[24] Benloucif A, Nguyen A T, Sentouh C, et al. Cooperative trajectory planning for haptic shared control between driver and automation in highway driving[J]. *IEEE Transactions on Industrial Electronics*, 2019, **66**(12): 9846 - 9857. DOI: 10.1109/TIE.2019.2893864.

[25] Nguyen A T, Sentouh C, Popieul J C. Driver-automation cooperative approach for shared steering control under multiple system constraints: Design and experiments[J]. *IEEE Transactions on Industrial Electronics*, 2017, **64**(5): 3819 - 3830. DOI: 10.1109/TIE.2016.2645146.

[26] Werling M, Kammel S, Ziegler J, et al. Optimal trajectories for time-critical street scenarios using discretized terminal manifolds[J]. *The International Journal of Robotics Research*, 2012, **31**(3): 346 - 359. DOI: 10.1177/0278364911423042.

无人驾驶路径跟踪控制计算方法

伍建伟[1,2] 孙蓓蓓[1] 傅琪迪[1] 刘彦豪[1]

([1]东南大学机械工程学院, 南京 211189)

([2]桂林电子科技大学机电工程学院, 桂林 541004)

摘要:考虑到自动驾驶车辆的轨迹跟踪控制缺乏统一的计算方法,特别是在误差计算、跟踪点确定和前馈控制器设计等方面,提出了完整的路径跟踪控制计算方法. 首先,根据车辆坐标系的动力学方程和路径跟踪模型,得到误差形式的控制方程. 然后,根据车辆当前的状态建立跟踪控制模型来获得车辆状态的偏差. 最后,根据动力学方程的特点,设计了具有前馈控制的线性二次调节控制器. 在此基础上,采用 MATLAB 语言开发程序,给出了仿真实例轨迹跟随控制的计算时间、抗干扰性和可靠性分析的仿真结果. 通过与文献实验结果对比,证明了所提出的计算方法是有效、可靠的,能够实现实时抗干扰的跟踪控制性能. 同时,通过有无前馈的仿真结果表明,引入前馈控制能够消除稳态误差,获得更好的控制性能.

关键词:路径跟踪;无人驾驶;前馈控制;线性二次调节控制器

中图分类号:U463.6